

# NLO QCD corrections to the production of $t\bar{t}Z$ in gluon fusion

Achilleas Lazopoulos and Kirill Melnikov

*Department of Physics and Astronomy, University of Hawaii,  
2505 Correa Rd. Honolulu, HI 96822*

Frank Petriello

*Department of Physics, University of Wisconsin, Madison, WI 53706*

## Abstract

We compute the  $\mathcal{O}(\alpha_s)$  QCD corrections to the partonic process  $gg \rightarrow t\bar{t}Z$  at the LHC. This partonic channel is the dominant component of the scattering process  $pp \rightarrow t\bar{t}Z$ , which will be important for measuring the  $t\bar{t}Z$  electroweak couplings. The  $\mathcal{O}(\alpha_s)$  corrections increase the total cross section by up to 75% for reasonable choices of the renormalization and factorization scales. Inclusion of these contributions decreases the residual scale dependence of the cross section coming from uncalculated higher order terms to  $\pm 5\%$ .

PACS numbers:

## I. INTRODUCTION

The discovery of the top quark in experiments at the Fermilab Tevatron established the validity of the Standard Model as a quantum field theory based on the gauge group  $SU(3) \times SU(2) \times U(1)$  with three generations of quarks [1]. Subsequently, the production cross section for  $t\bar{t}$  pairs in proton anti-proton collisions was measured with good precision and the value of the top quark mass was established to nearly the percent level [2]. Very recently, the first observation of single top production was reported [3].

While the above studies are important milestones in top quark physics, these measurements probe only a limited subset of top quark properties. The process  $p\bar{p} \rightarrow t\bar{t}$  at the Tevatron is sensitive to the top quark mass and color charge. The decay  $t \rightarrow Wb$  is marginally sensitive to the  $tWb$  coupling. Other important properties of the top quark, such as its couplings to the  $Z$ -boson and the photon and its Yukawa coupling, cannot currently be directly accessed experimentally. These couplings are sensitive probes of new physics effects; in particular, the  $Zt\bar{t}$  coupling is affected by tree-level mixing with additional  $Z'$  gauge bosons and vector-like fermions.

While the best place to perform detailed studies of the top quark is the International Linear Collider, useful information about the top quark couplings to electroweak gauge bosons and the Higgs boson can be obtained from the LHC where the processes  $pp \rightarrow t\bar{t}H$ ,  $pp \rightarrow t\bar{t}Z$  and  $pp \rightarrow t\bar{t}\gamma$  can be observed. However, in order to use those observations, accurate theoretical predictions for the signal and background events are required. Since the cross sections for all signal processes scale as  $\sigma_{\text{LO}} \sim \alpha_s^2$  at leading order in the QCD perturbative expansion, there is significant uncertainty in the normalization of the leading order cross section. To remove this theoretical error, a computation of the cross section through next-to-leading order (NLO) in  $\alpha_s$  is required.

Recently, the possibility of measuring the top quark couplings to the photon and the  $Z$ -boson at the LHC was studied in detail [4, 5]. The study in Ref. [4] required that the  $Z$ -boson decays leptonically, and allowed for either zero or one leptonic  $W$  boson decay. Both channels have a reasonable signal to background ratio. It was pointed out in Ref. [5] that further improvements can be achieved by considering the decay  $Z \rightarrow \nu\bar{\nu}$ . The background processes to  $pp \rightarrow t\bar{t}Z$  and  $pp \rightarrow t\bar{t}\gamma$  scale with a high power of  $\alpha_s$ ,  $\sigma_{\text{bckg}} \sim \alpha_s^n$ ,  $n \geq 2$ . Consequently, theoretical predictions for these processes are quite uncertain. Nevertheless, as pointed out in Refs. [4, 5], it may be possible to experimentally study them in signal-free regions to control the background normalization. In principle, this technique allows the extraction of the  $t\bar{t}Z$  and  $t\bar{t}\gamma$  couplings from the  $t\bar{t}Z(\gamma)$  cross section measurements, if not for the normalization uncertainty in the signal cross sections themselves associated with unknown QCD corrections. It was shown in Ref. [4] that this uncertainty is a limiting factor in extracting anomalous  $t\bar{t}Z$  couplings in the leptonic  $Z$  decay channels.

In this paper we take the first step towards computing the NLO QCD corrections to  $t\bar{t}Z$  production at the LHC by considering the  $gg \rightarrow t\bar{t}Z$  partonic subprocess. We focus on this reaction for two reasons. First, gluon collisions at the LHC are important because of the large gluon luminosity. This can be seen already at leading order where the  $gg \rightarrow t\bar{t}Z$  subprocess gives approximately 60% of the full result. Second, the computation of NLO QCD corrections to the  $gg \rightarrow t\bar{t}Z$  subprocess is technically more involved than the corresponding computation for quark anti-quark annihilation channels. It can also be expected that NLO QCD corrections to  $gg \rightarrow t\bar{t}Z$  are larger than corrections to  $q\bar{q} \rightarrow t\bar{t}Z$ , since the color charge of gluons is larger than that of quarks. For these reasons we believe that the computation

presented in this paper gives a good idea about the importance of  $\mathcal{O}(\alpha_s)$  corrections to the full  $pp \rightarrow t\bar{t}Z$  process. However, a detailed study of how NLO QCD influences the extraction of the  $t\bar{t}Z$  coupling requires the inclusion of the  $q\bar{q}$  and  $qg$  channels. We plan to extend our computation to incorporate the quark-initiated production processes in the near future.

Our paper is organized as follows. In the next Section we introduce our notation and briefly discuss the calculation of the leading order cross section. Section III describes the computation of the  $\mathcal{O}(\alpha_s)$  corrections. In Section IV, numerical results are presented and discussed. We conclude in Section V.

## II. NOTATION AND THE LEADING ORDER CROSS SECTION

We consider the process  $p(P_1) + p(P_2) \rightarrow t\bar{t}Z$ . The factorization theorems for hard scattering processes in QCD allow us to write

$$d\sigma = \sum_{ij} \int_0^1 dx_1 dx_2 f_i^1(x_1) f_j^2(x_2) d\sigma_{ij \rightarrow t\bar{t}Z}(x_1 x_2 S), \quad (1)$$

where  $f_{i,j}^{(1,2)}(x_{1,2})$  are the parton densities that give the probability to find parton  $i(j)$  in the proton 1(2) with momentum  $p_{i(j)} = x_{1(2)}P_{1(2)}$ . The center-of-mass energy squared of the proton-proton collision is introduced in Eq. (1),  $S = 2P_1 \cdot P_2$ . In this paper, we only consider gluon collisions at the LHC, so we set  $i = j = \text{gluon}$  in Eq. (1) and use  $\sqrt{S} = 14$  TeV.

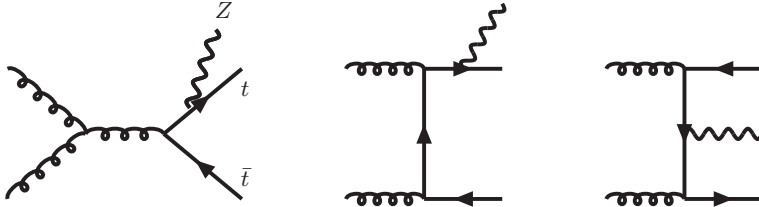


FIG. 1: Sample diagrams for  $gg \rightarrow t\bar{t}Z$  appearing at leading order.

At leading order in the  $\alpha_s$  expansion, there are eight Feynman diagrams that contribute to  $gg \rightarrow t\bar{t}Z$ ; some examples are shown in Fig.1. The computation of the leading order cross section is straightforward. We use QGRAF [6] to generate the relevant Feynman diagrams and then MAPLE and FORM [7] to manipulate this output. Throughout the paper we set  $m_t = 170.9$  GeV,  $m_Z = 91.18$  GeV, and  $m_W = 80.45$  GeV. For the coupling of the  $Z$ -boson to quarks, we employ

$$Zqq : i\sqrt{\frac{8m_W^2 G_F}{\sqrt{2} \cos^2 \theta_W}} (g_v^q + g_a^q \gamma_5), \quad (2)$$

where  $g_v^q = \frac{T_3^q}{2} - Q_q \sin^2 \theta_W$ ,  $g_a^q = -\frac{T_3^q}{2}$ ,  $\sin^2 \theta_W = 1 - m_W^2/m_Z^2 = 0.2215$  is the sine squared of the electroweak mixing angle,  $T_3^q$  is the weak isospin of the quark  $q$ ,  $Q_q$  is the electric charge of the quark  $q$  in units of the proton charge and  $G_F$  is the Fermi constant. Numerical results for the leading order cross section are reported in Section IV.

### III. NEXT-TO-LEADING ORDER COMPUTATION

We now discuss the computation of the next-to-leading order corrections to the partonic process  $gg \rightarrow t\bar{t}Z$ . Three distinct contributions should be considered: virtual corrections to the leading order process  $gg \rightarrow t\bar{t}Z$ , the real emission corrections  $gg \rightarrow t\bar{t}Z + g$ , and the renormalization of the leading order cross section.

We first consider the computation of the virtual corrections to  $gg \rightarrow t\bar{t}Z$ . There are 162 diagrams that contribute at next-to-leading order. Some examples of these one-loop diagrams are shown in Fig. 2. These diagrams fall into two categories:

- diagrams in which the  $Z$ -boson couples to the top quark, such as the first two shown in Fig. 2;
- diagrams in which the  $Z$ -boson couples to an internal quark propagator, such as the final one in Fig. 2.

The first class contains contributions proportional to the coupling constant combinations  $(g_v^t)^2$  and  $(g_a^t)^2$ . Diagrams in this class can be computed with standard  $d$ -dimensional Dirac algebra, using the anti-commutation prescription for  $\gamma_5$ . The second class contains contributions proportional to  $g_v^t g_v^q$  and  $g_a^t g_a^q$ , where  $q$  denotes any of the six quarks. The diagrams in this class contain products of two Dirac traces with single  $\gamma_5$  terms, leading to contributions containing a product of two Levi-Civita tensors. Although this second set of diagrams is finite, we use the  $d$ -dimensional prescription for  $\gamma_5$  described in Ref. [8] for calculational convenience in the intermediate steps.

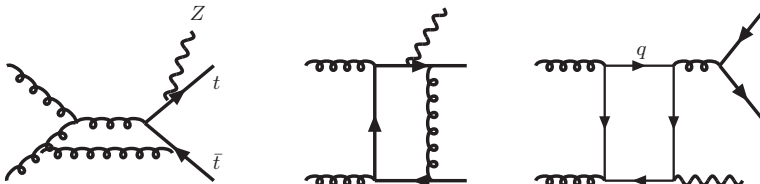


FIG. 2: Sample diagrams for the  $\mathcal{O}(\alpha_s)$  virtual corrections to  $gg \rightarrow t\bar{t}Z$ .

To compute the virtual corrections, we employ the method described in Ref. [9]. We summarize here the salient features of this technique. Further details can be found in Ref. [9]. We compute the square of the scattering amplitude, summing over the fermion spins and polarizations of gluons and the  $Z$ -boson. For each one-loop diagram interfered with the full Born amplitude, we perform the integration over the loop momentum and arrive at an integral over Feynman parameters. The integration over Feynman parameters cannot be computed numerically because it diverges. While the ultraviolet divergencies factorize after the integration over the loop momentum and therefore have no effect on the integration over Feynman parameters, the infrared and collinear singularities appear when certain Feynman parameters approach boundary values. To have a representation of the integrals suitable for numerical evaluation, we must extract the infrared and collinear singularities. We accomplish this using the method of sector decomposition [10]. However, even after these divergencies are extracted, it is not possible to perform the Feynman parameter integrations numerically because there are singularities inside the integration region coming from internal loop thresholds. These singularities are avoided by deforming the integration

contour into the complex plane following the suggestion in Ref. [11]. Once infrared and collinear singularities are extracted and the integration contour is deformed, we obtain representations of the Feynman parametric integrals suitable for numerical integration. This integration is performed using the adaptive Monte Carlo integration algorithm VEGAS [12] as implemented in the CUBA library [13].

We briefly comment here on the stability of the numerical integration. In principle, after extracting infra-red and collinear singularities and deforming the contour into the complex plane, the integration should be numerically stable. For most phase space points that we consider, we find this to be the case. However, there are situations where straightforward application of the algorithm described in [9] leads to numerical instabilities. These instabilities typically occur when the sector decomposition procedure “overdoes” the extraction of singularities, splitting the integral into too many sectors which each contain unphysical singularities. Problems of these type occur typically in the evaluation of five-point functions. We handle these problematic cases by choosing a more sophisticated parameterization of the original Feynman integral. For example, if in a five-point function two propagators  $D_{1,2}$  never become singular, it is beneficial to combine them first into a single propagator:

$$\frac{1}{D_1 D_2} = \int_0^1 \frac{d\xi}{D(\xi)^2}, \quad D(\xi) = \xi D_1 + (1 - \xi) D_2. \quad (3)$$

Using this and similar techniques we are able to obtain a stable numerical representation for all virtual diagrams that contribute to the  $gg \rightarrow t\bar{t}Z$  process.

In order to arrive at a finite result at next-to-leading order, renormalization is required. We employ the  $\overline{\text{MS}}$  renormalization constants for the QCD coupling  $\alpha_s$  with five active flavors; the top quark contribution to the coupling constant renormalization is decoupled through a zero-momentum subtraction. In addition, we renormalize the top quark wave function and the top quark mass on shell. No other renormalization constants or counter-terms are required to render  $\mathcal{O}(\alpha_s)$  corrections to  $gg \rightarrow t\bar{t}Z$  process ultraviolet finite.

We must also compute the real emission diagrams corresponding to the process  $gg \rightarrow t\bar{t}Z + g$ . There are 50 such diagrams. When the gluon in the final state is soft or collinear to the gluons in the initial state, the matrix element for  $gg \rightarrow t\bar{t}Z + g$  process becomes singular. To compute the corresponding contribution to the cross section, we split the phase-space for real gluon emission into soft, collinear and hard parts, using the two cutoff slicing method [14]. The singularities that originate from collinear gluon emission are removed using the  $\overline{\text{MS}}$  renormalization of the parton distribution functions. The computation of real emission corrections to  $gg \rightarrow t\bar{t}Z$  using the two cutoff slicing method is analogous to the computation of real emission corrections for the  $gg \rightarrow t\bar{t}H$  process described in [15], where many details can be found.

## IV. RESULTS

We now present the results of our computation. For all numerical results reported in this paper, we set the renormalization scale  $\mu_r$  and the factorization scale  $\mu_f$  equal to a common scale:  $\mu_r = \mu_f = \mu$ . We employ the MRST parton distribution functions [16] at the appropriate order in the perturbative expansion. We have applied a number of checks to our calculation.

1. We have compared the leading order cross-section obtained with our code with the result of a similar computation using the program MadEvent [17] and have found complete agreement.
2. The divergent parts of the NLO virtual correction to  $gg \rightarrow t\bar{t}Z$  can be expressed in a simple analytic form, as explained in detail in [15]. We have checked that our results satisfy this check.
3. We have checked that all divergences cancel once the real emission processes, the collinear counterterms, the renormalization constants, and the virtual corrections are combined.
4. An important check of our NLO virtual result is provided by its independence of the size of the contour deformation.
5. Finally, we have implemented all parts of the computation in several different codes that agree for all observables studied.

$\mu$	$\sigma_{\text{LO}}$ , fb	$\sigma_{\text{NLO}}$ , fb	$K = \sigma_{\text{NLO}}/\sigma_{\text{LO}}$
$\mu_0/8$	1046	587	0.56
$\mu_0/4$	738	740	1.00
$\mu_0/2$	537	739	1.38
$\mu_0$	400	695	1.74
$2\mu_0$	305	618	2.03

TABLE I: The cross section at leading and next-to-leading order for various values of the renormalization and factorization scales. The numerical error on all numbers presented is 1% or better.

We begin with the total cross section. The results of our calculation are summarized in Table I. We show there the total cross section computed through leading and next-to-leading order for the five values of the scale  $\mu = (1/8, 1/4, 1/2, 1, 2)\mu_0$ , where  $\mu_0 = (2m_t + m_Z)$ . For the QCD coupling constant, we use values consistent with the MRST parton densities at leading and next-to-leading order [16] at  $\mu = m_Z$  and evolve these values using the beta-function at the appropriate order in the perturbative expansion. We see from Table I that the leading order result changes by more than a factor of 3 when the scale  $\mu$  changes between its minimal and maximal values. This suggests significant  $\mathcal{O}(\alpha_s)$  corrections. Indeed, as clearly seen from the last column in Table I, the NLO QCD corrections are large. They change the leading order corrections by up to a hundred percent, depending on the value of the scale  $\mu$ . The dependence of the next-to-leading order cross section on the scale  $\mu$  is significantly reduced; when  $\mu$  is varied between  $\mu_0/8$  and  $2\mu_0$ ,  $\sigma_{\text{NLO}}$  changes by only a factor of 1.25.

While formally all values of the renormalization and factorization scales are allowed, the best predictions for physical quantities at low orders in perturbation theory are obtained when the scales are set to values suggested by the physics of the problem. The typical partonic center-of-mass energies leading to the  $t\bar{t}Z$  final state are moderate,  $\sqrt{s_{gg}} \lesssim 10^3$  GeV, and the typical transverse momenta for the  $Z$ -boson and top quarks are 100 – 200 GeV. It seems reasonable to choose scales comparable to the typical transverse momenta. This suggests setting  $\mu \sim \text{few} \times 100$  GeV. Since  $\mu_0 \sim 2m_t + m_Z \sim 450$  GeV, we consider

$\mu = [\mu_0/4, \mu_0]$  as a sensible range for the variation of the renormalization and factorization scales. As follows from Table I, in this range  $\sigma_{\text{LO}}(\sigma_{\text{NLO}})$  changes by about  $\pm 30\%$  ( $\pm 5\%$ ) if measured from the central value  $\mu = \mu_0/2$ .

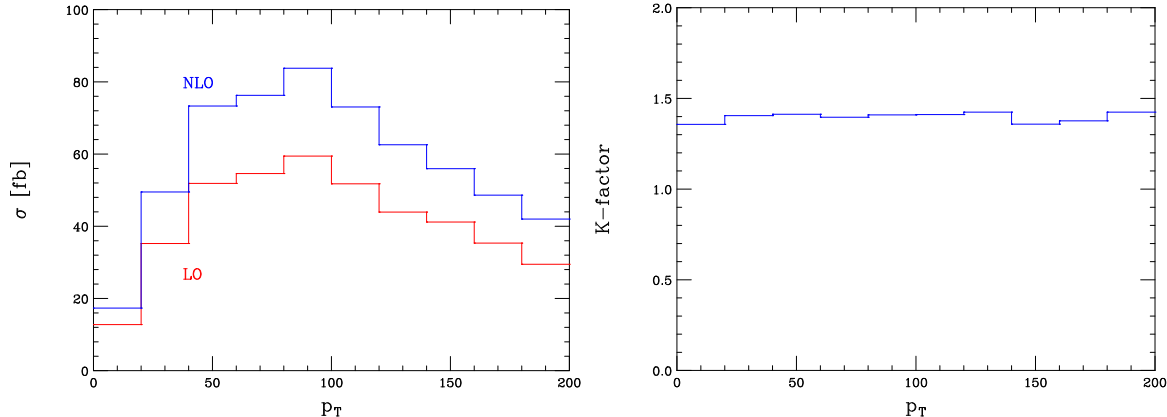


FIG. 3: Left panel: the transverse momentum distribution of the  $Z$ -boson at leading order and next-to-leading order in  $\alpha_s$ . Right panel: the dependence of the  $K$ -factor defined as  $K = d\sigma_{\text{NLO}}/d\sigma_{\text{LO}}$  on the transverse momentum of the  $Z$ -boson. We set  $\mu = \mu_0/2$  in both plots.

As pointed out in Ref. [4, 5], the signal-to-background ratio for  $pp \rightarrow t\bar{t}Z$  production is improved if a cut on the transverse momentum of the  $Z$ -boson  $p_{\perp}(Z)$  is imposed since many background processes decrease faster than the signal when  $p_{\perp}(Z)$  increases. It is therefore interesting to study the effect of the NLO QCD corrections on the  $p_{\perp}(Z)$  distribution. In the left panel of Fig. 3 we show the transverse momentum distribution of the  $Z$ -boson at leading order and next-to-leading order in the strong coupling constant. We combine events in 20 GeV bins. We set the factorization and renormalization scales to  $\mu = \mu_0/2$ . While the QCD corrections change the distribution significantly, they affect only the overall normalization. This is clearly seen from the right panel of Fig. 3, where the  $K$ -factor defined as  $K = d\sigma_{\text{NLO}}/d\sigma_{\text{LO}}$  is shown.

We have only considered QCD corrections to the gluon fusion subprocess in  $pp \rightarrow t\bar{t}Z$ . Given the large gluon-gluon luminosity at the LHC and the fact that QCD corrections to gluon initiated processes are usually larger than those for quark-initiated, this seems to be a reasonable first step towards the complete NLO QCD computation. However, it is premature to discuss in detail how the NLO QCD corrections affect the analyses in Ref.[4, 5]. We make one comment here. In Refs.[4, 5],  $\sigma(pp \rightarrow t\bar{t}Z)$  was computed with the renormalization and factorization scales set equal to the top quark mass. As follows from Table I, for such renormalization and factorization scales the NLO QCD corrections for the  $gg \rightarrow t\bar{t}Z$  subprocess are about 30 percent. Assuming that QCD corrections to quark initiated process are somewhat smaller, NLO QCD corrections of about 20% to  $pp \rightarrow t\bar{t}Z$  for  $\mu = m_t$  can be expected. The NLO QCD corrections are positive and enhance the signal cross section, leading to a decrease in the luminosity required to probe the  $t\bar{t}Z$  coupling. The NLO QCD computation also reduces the theoretical uncertainty of the signal cross section coming from uncalculated higher order corrections. We estimate that the residual scale uncertainty is  $\pm 5\%$  by varying the scale between  $\mu_0/4$  and  $\mu_0$ .

## V. CONCLUSIONS

In this paper we presented the NLO QCD corrections to gluon-initiated production of  $t\bar{t}Z$  at the LHC. This is a first step towards the full NLO QCD calculation of  $pp \rightarrow t\bar{t}Z$  needed to study electroweak top quark couplings. For reasonable choices of the renormalization and factorization scales, the QCD corrections can be up to 75%. The remaining theoretical uncertainty in the cross section after inclusion of the NLO corrections is estimated to be  $\pm 5\%$ . The NLO QCD contributions are independent of the transverse momentum of the  $Z$ -boson.

In the future, we plan to extend this computation to include the quark anti-quark annihilation and quark-gluon partonic scattering processes. It will then be possible to incorporate the improved knowledge of the signal processes into the analysis of Ref. [4, 5].

**Acknowledgments** K.M. would like to thank the Galileo Galilei Institute for Theoretical Physics for their hospitality, and the INFN for partial support during the completion of this work. K.M. and A.L. are supported in part by the DOE grant DE-FG03-94ER-40833, Outstanding Junior Investigator Award and by the Alfred P. Sloan Foundation. F.P. is supported by the DOE grant DE-FG02-95ER40896, Outstanding Junior Investigator Award, by the University of Wisconsin Research Committee with funds provided by the Wisconsin Alumni Research Foundation, and by the Alfred P. Sloan Foundation.

- 
- [1] F. Abe *et al.* [CDF Collaboration], Phys. Rev. Lett. **74**, 2626 (1995) [arXiv:hep-ex/9503002]; S. Abachi *et al.* [D0 Collaboration], Phys. Rev. Lett. **74**, 2632 (1995) [arXiv:hep-ex/9503003].
  - [2] M. A. Pleier, for the CDF and D0 Collaborations, arXiv:0709.2665 [hep-ex].
  - [3] A. Garcia-Bellido [D0 collaboration], arXiv:0706.0037 [hep-ex]; B. Stelzer [CDF Collaboration], arXiv:0706.0282 [hep-ex].
  - [4] U. Baur, A. Juste, L. H. Orr and D. Rainwater, Phys. Rev. D **71**, 054013 (2005) [arXiv:hep-ph/0412021].
  - [5] U. Baur, A. Juste, D. Rainwater and L. H. Orr, Phys. Rev. D **73**, 034016 (2006) [arXiv:hep-ph/0512262].
  - [6] P. Nogueira, J. Compt. Phys. **105**, 279 (1993).
  - [7] J. A. M. Vermaseren, arXiv:math-ph/0010025.
  - [8] S. A. Larin, Phys. Lett. B **303**, 113 (1993) [arXiv:hep-ph/9302240].
  - [9] A. Lazopoulos, K. Melnikov and F. Petriello, Phys. Rev. D **76**, 014001 (2007) [arXiv:hep-ph/0703273].
  - [10] T. Binoth and G. Heinrich, Nucl. Phys. B **585**, 741 (2000) [arXiv:hep-ph/0004013]. For earlier work see also M. Roth and A. Denner, Nucl. Phys. **B479**, 495 (1996)[arXiv:hep-ph/9605420]; K. Hepp, Commun. Math. Phys. **2**, 301 (1966).
  - [11] D. E. Soper, Phys. Rev. Lett. **81**, 2638 (1998) [arXiv:hep-ph/9804454]; D. E. Soper, Phys. Rev. D **62**, 014009 (2000) [arXiv:hep-ph/9910292]; D. E. Soper, Phys. Rev. D **64**, 034018 (2001) [arXiv:hep-ph/0103262]; Z. Nagy and D. E. Soper, Phys. Rev. D **74**, 093006 (2006) [arXiv:hep-ph/0610028].
  - [12] G. P. Lepage, J. Comp. Phys. **27**, 192 (1978); Cornell University report CLNS-80/447, (1980).
  - [13] T. Hahn, Comput. Phys. Commun. **168**, 78 (2005) [arXiv:hep-ph/0404043].



- [14] B. W. Harris and J. F. Owens, Phys. Rev. D **65**, 094032 (2002) [arXiv:hep-ph/0102128].
- [15] W. Beenakker, S. Dittmaier, M. Kramer, B. Plumper, M. Spira and P. M. Zerwas, Nucl. Phys. B **653**, 151 (2003) [arXiv:hep-ph/0211352]; S. Dawson, C. Jackson, L. H. Orr, L. Reina and D. Wackerth, Phys. Rev. D **68**, 034022 (2003) [arXiv:hep-ph/0305087].
- [16] A.D. Martin, R.G. Roberts, W.J. Stirling and R.S. Thorne, Eur. Phys. J. **C23**, 73 (2002); Phys. Lett. **B531**, 216 (2002).
- [17] F. Maltoni and T. Stelzer, JHEP **0302**, 027 (2003) [arXiv:hep-ph/0208156].